RANS Simulations of a Small Turbine Cascade

VIVIEN S. DJANALI, K.C. WONG and S.W. ARMFIELD
School of Aerospace, Mechanical and Mechatronics Engineering
The University of Sydney
Sydney, NSW 2006
AUSTRALIA

Abstract: - Modelling a small turbine is of interest due to the rapid development of small jet engines for model aircraft and UAVs. Because of its size, a small jet engine has small air mass flow rate, low component pressure ratios, high rotational speed and relatively low Reynolds number. The Reynolds number has a major effect on the boundary layer characteristics, shear stresses and losses in the turbine. At low Reynolds number, boundary layers tend to be laminar or in transition and less resistant to separation. Thus, this research is performed to predict separation on the small turbine rotor blade at various Reynolds numbers and turbulence intensity levels. Transitional flows were simulated using the three-equation k_T-k_L-ω model of Walters and Leylek, which includes the effect of natural transition and bypass transition. The simulation results show separation appears at all flow condition, and thus underline that small turbine rotors are highly susceptible to separation.

Key-Words: - Small turbine, Transitional flow, RANS simulation, Low Reynolds number, Separation

1 Introduction

Jet engines were developed more than 70 years ago. Since then, many efforts have been made to improve the performance, increase the efficiency and reduce the size and the weight of the engine. In the 1990's, researcher started to design small jet engines due to the high demand for model airplane and Unmanned Aerial Vehicle (UAV) applications. Many types of small jet engines are currently being manufactured and sold throughout the world. However, these engines have very low efficiencies and high specific fuel consumptions.

To design a small jet engine is not as simple as scaling a big jet engine. A small jet engine has much lower efficiency than the standard-size jet engine used in aircraft. Because of its size, a small jet engine has very small air mass flow rate, low component pressure ratios, high rotational speed and relatively low Reynolds number. The Reynolds number has a major effect on the boundary layer characteristics, shear stresses and losses in the engine's components. At low Reynolds number, boundary layers are laminar and less resistant to separation.

Researchers and manufacturers need to focus on redesigning a small jet engine, not just scaling the jet engine. However, very limited research on small jet engines has been undertaken. Many small jet engine manufacturers design their engine components only by trial and error; a limited and expensive approach. Therefore, it is useful to analyse a small jet engine using simulation in order to optimise the engine components design.

One of the main components of a jet engine is the turbine. Currently, the turbine of a small jet engine has much lower efficiency than the turbine of a standard-size jet engine which reaches approximately 90% [1]. According to Frank Turbine [2], small jet engine type Turbojet 66 has a turbine efficiency around 75%. The low Reynolds number on a turbine rotor blade passage means that it has mostly laminar boundary layer or transition flow on the suction side of the blade, and as a result is more susceptible to separation in the blade passage. The transition that occurs on a small turbine rotor is more likely to be a bypass transition, due to its high free stream turbulence intensity level. In bypass transition, the instabilities grow rapidly induced by the high disturbances of the free stream.

The low Reynolds number flow on a small turbine rotor is similar to the flow on a low pressure turbine (LPT) blade of commercial aircraft turbines. The LPT blade cascade experiment of Lake et al. [3] showed a separation zone from 60% of the axial chord to the trailing edge, for Re = 50,000 and inlet turbulence intensity of 1%. The experiment also showed the separation zones were smaller at higher Reynolds numbers and higher turbulence intensities.

An experiment with the same turbulence intensity level was conducted by Dorney et al. [4]. For Re = 43,000, the onset of separation is at 60% of the axial chord with no reattachment downstream. For Re = 86,000, the flow separates at 72% of the axial chord and reattaches at 87% of the axial chord. Since reattachment occurs, the separation region at Re = 86,000 is smaller than that at the lower Reynolds number, causing less losses in the blade passage.

Because most of the flow of a small turbine and a low pressure turbine are in transition, studying and modelling transitional flow is increasingly important. Reynolds Averaged Navier Stokes turbulence models, which perform well in fully turbulent flow, are found to be unable to capture separation in transitional flows of this type. Even though low Reynolds number models can qualitatively depict the transition process, these models still do not perform satisfactorily [5]. Therefore, many studies have been carried out to develop transition models. One way to simulate transitional flow is by modifying the low Reynolds number models to include an intermittency factor, either obtained empirically or calculated using an intermittency transport equation ([6], [7], [8] and [9]). Wang and Perot [10] predict transition boundary layers using the turbulent potential model. Another way to simulate transition is by calculating the fluctuation growth of both laminar and turbulent kinetic energy, as in the models developed by Walters and Leylek [11], [12].

As a part of a design optimisation project for small jet engines, this study is conducted to predict separation for the transitional boundary layer of a small turbine rotor blade using a RANS model. Although a small turbine rotor blade profile has more favourable pressure gradient than that of a LPT blade profile, a small turbine rotor is operating at lower Reynolds number. Thus, this study will be useful as a preliminary investigation of the losses on a small turbine for further design optimisation.

2 Simulation Method

2.1 Turbulence Models

The three-equation k_T-k_L-ω model developed by Walters and Leylek [12] was used to simulate the transitional flow on a small turbine rotor cascade. The three transport equations are:

$$\frac{Dk_T}{Dt} = P_{k_T} + R + R_{NAT} - \varepsilon - D_T + \frac{\partial}{\partial x_j}\left[\left(\nu + \frac{\alpha_T}{\sigma_k}\right)\frac{\partial k_T}{\partial x_j}\right], \quad (1)$$

$$\frac{Dk_L}{Dt} = P_{k_L} - R - R_{NAT} - D_L + \frac{\partial}{\partial x_j}\left[\nu\frac{\partial k_L}{\partial x_j}\right], \quad (2)$$

$$\frac{D\omega}{Dt} = P_\omega + C_{\omega R}\frac{\omega}{k_T}(R + R_{NAT}) - C_{\omega 2}\omega^2 + C_{\omega 3} f_\omega \alpha_T \left(\frac{\lambda_{eff}}{\lambda_T}\right)^{4/3}\frac{\sqrt{k_T}}{d^3} + \frac{\partial}{\partial x_j}\left[\left(\nu + \frac{\alpha_T}{\sigma_\omega}\right)\frac{\partial \omega}{\partial x_j}\right], \quad (3)$$

where k_T is the turbulence kinetic energy, k_L is the laminar kinetic energy and ω is the specific dissipation rate. The kinematic Reynolds stress tensor is calculated as:

$$-\overline{u_i u_j} = \nu_{TOT}\left(\frac{\partial U_i}{\partial x_j} + \frac{\partial U_j}{\partial x_i}\right) - \frac{2}{3}k_{TOT}\delta_{ij}, \quad (4)$$

with $k_{TOT} = k_T + k_L$.

This model is a single-point low Reynolds number model that calculates the laminar and turbulence kinetic energy over the full domain, with the eddy viscosity obtained as a function of k_T, k_L and ω, with no intermittency factor used. The effect of natural and bypass transition are also included in this model. Moreover, it is developed to be used with y^+ of less than one. This model has been tested on a highly-loaded turbine cascade, a compressor-like flat plate and a circular cylinder, and has showed good agreement with experimental data at various free stream turbulence intensity levels ([12], [13] and [14]).

2.2 Computational Details

The turbine blade used in this study was an Artesjet KJ66 turbine rotor blade profile with stagger angle of 37.5^0. The relative velocity inlet angle was set at 20^0 to the axial direction. Two-dimensional steady simulations were performed using FLUENT version 6.2.16. The three-equation model was implemented in FLUENT using User-Defined Functions (UDFs) and User-Defined Scalars (UDSs). A segregated-implicit solver and SIMPLE algorithm for the pressure-velocity coupling were used. The diffusion terms were evaluated using second-order central differencing and the convective terms were evaluated using a first-order discretisation scheme.

The computational domain was generated in Gambit using a structured quadrilateral mesh and contained in total 68,030 cells, as shown in Figure 1. An O-type mesh, containing 888 x 60 cells, was used in the near blade region and an H-type mesh was used in the far field. The average value of y^+ for the wall adjacent node was 0.1 and the maximum y^+ value was 0.4, with approximately 20 cells in the boundary layer.

Periodic boundary conditions were used on the

region between the blades. Inlet boundary conditions for k_T and ω were determined as for the standard turbulence model and k_L was set to zero. In addition, wall boundary conditions for k_T, k_L and ω were set to zero flux.

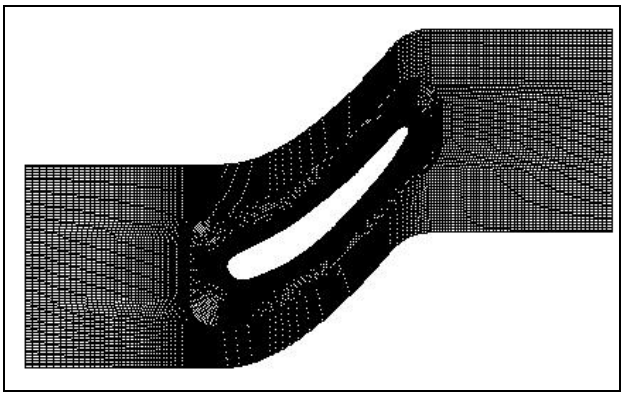

Fig.1 Computational domain

3 Results

Simulations were performed at various Reynolds number, based upon the relative inlet velocity (U_∞) and the axial chord length (L), of 14,000, 23,000 and 32,000. These Reynolds numbers were chosen as the initial prediction of the turbine rotor flow, since no experimental data is available yet. The inlet turbulence intensities (Tu_∞) were set to 3% and 10%. The simulation results show that separation occurs at all Reynolds numbers and turbulence intensity levels, as shown on Table 1. The wake region was observed on the suction side of the blade near the trailing edge. The wake extends to the outlet of the cascade, causing high losses in the blade passage. The wake region is smaller for flow with higher turbulence intensity levels.

Table 1 Numerical simulation results

Reynolds Number		Tu_∞ = 3%	Tu_∞ = 10%
14,000	Separation	0.584	0.873
	Reattachment	-	-
	2nd separation	-	-
23,000	Separation	0.61	0.91
	Reattachment	0.685	-
	2nd separation	0.751	-
32,000	Separation	0.603	0.913
	Reattachment	0.708	-
	2nd separation	0.725	-

The result plotted in Fig.2 shows that the separation point for increasing Reynolds numbers at fixed inlet turbulence intensity barely changes. On the other hand, the separation point is very sensitive to the inlet turbulence intensity level, with a separation at about 60% and 90% of the axial chord length for Tu_∞ = 3% and 10%, respectively.

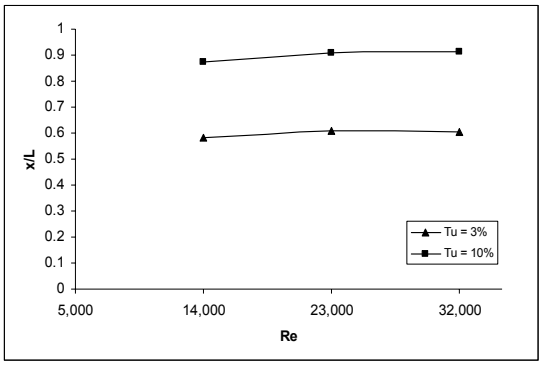

Fig.2 The onset of separation for various flow conditions

For Tu_∞ = 3%, the simulation predicts separation only with no reattachment downstream at Re = 14,000. For higher Reynolds number, separation and reattachment occur followed by second separation near the trailing edge. Fig.3 shows the non-dimensional tangential velocity along the first cell of the suction side of the blade. Negative values of the non-dimensional velocity represent the separation region, while zero value represents the point of separation, reattachment or second separation. The Mach number contours for various Reynolds number at Tu_∞ = 3% are shown in Fig. 4 to Fig.6.

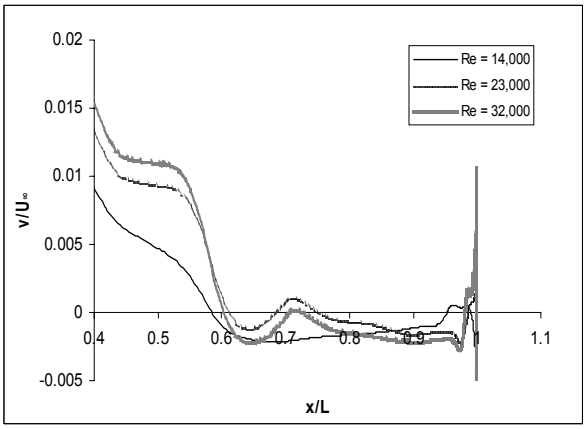

Fig.3 Non-dimensional velocity along the suction side for Tu_∞ = 3%

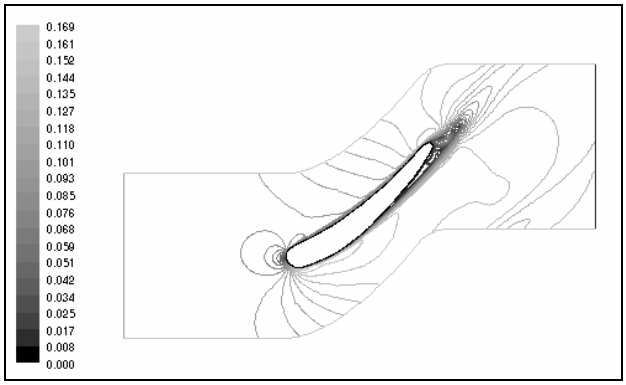

Fig.4 Mach number contours
for Re = 14,000, Tu_∞ = 3%

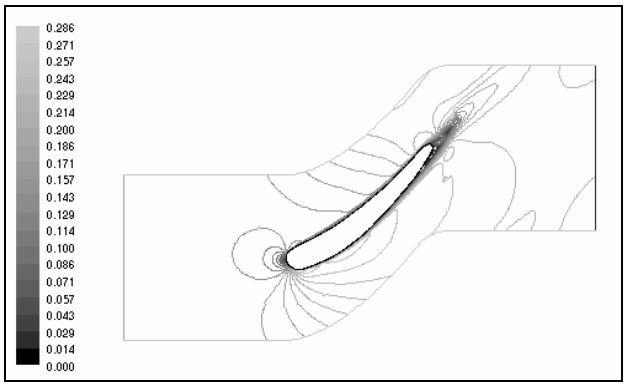

Fig.5 Mach number contours
for Re = 23,000, Tu_∞ = 3%

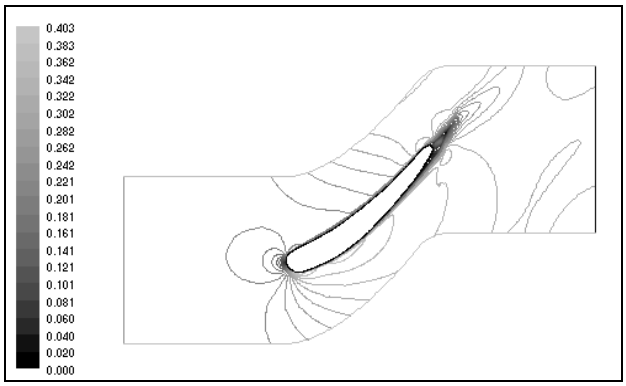

Fig.6 Mach number contours
for Re = 32,000, Tu_∞ = 3%

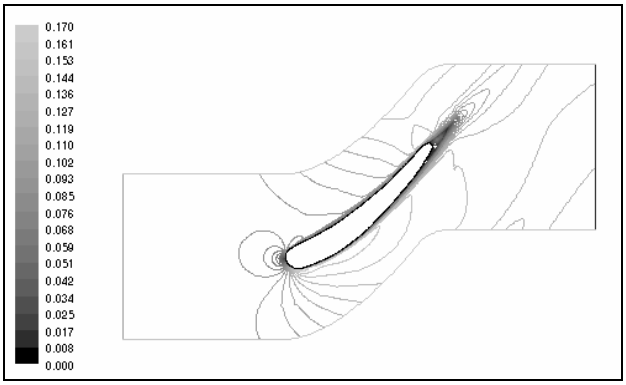

Fig.7 Mach number contours
for Re = 14,000, Tu_∞ = 10%

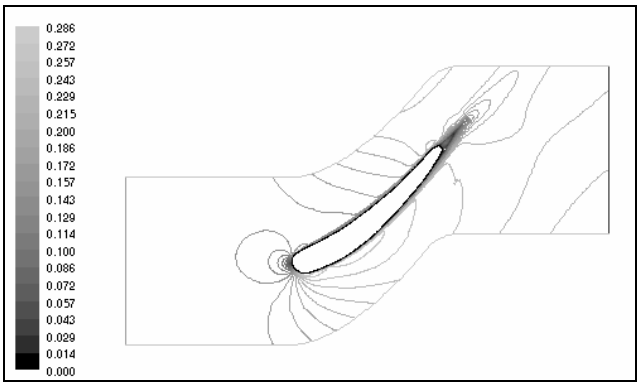

Fig.8 Mach number contours
for Re = 23,000, Tu_∞ = 10%

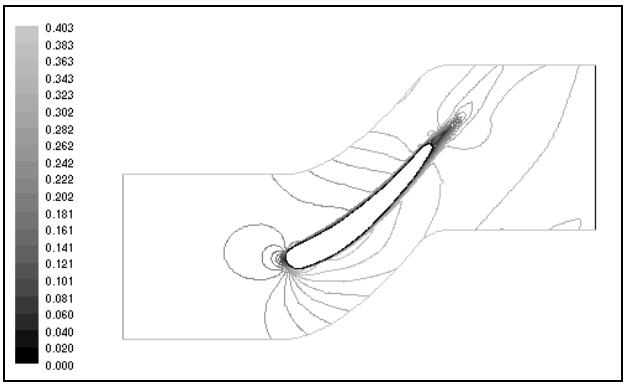

Fig.9 Mach number contours
for Re = 32,000, Tu_∞ = 10%

For Tu_∞ = 10%, the separation point moves towards the trailing edge. At higher inlet turbulence intensity level, the flow has more kinetic energy to delay the separation. The flow separates near the trailing edge and has no opportunity to reattach, as shown in Fig.7 to Fig.9.

Fig.10 shows the non-dimensional tangential velocity along the first cell of the suction side of the blade for Tu_∞ = 10%. Negative values of the non-dimensional velocity represent the separation region, while zero value represents the point of separation.

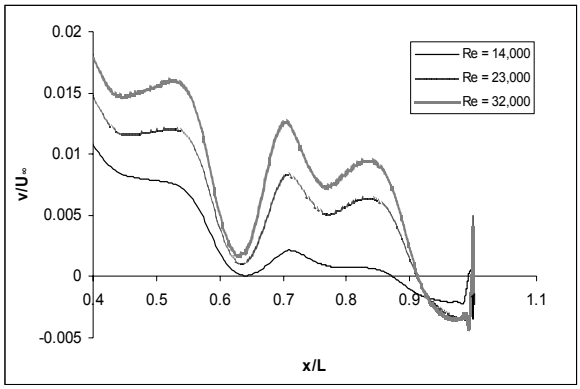

Fig.10 Non-dimensional velocity along the suction side for $Tu_\infty = 10\%$

4 Conclusion

The simulations capture the separation at all flow conditions. The separation occurs early at nearly half of the blade for $Tu_\infty = 3\%$, with reattachment and second separation downstream for Re = 23,000 and 32,000. For higher free stream turbulence intensity level, the separation is delayed, due to the higher kinetic energy. These results suggest that the flow in a small turbine rotor is very susceptible to separation. Since no experimental data are available, these simulation results can not be validated yet. Experimental data are needed for the future work of investigating a small turbine. However, these results have substantially depicted the basic separated flow on a small turbine rotor.

References:

[1] Rolls-Royce Ltd., *The Jet Engine*, Derby, 1969.

[2] Frank, I., Modellstrahlturbine Turbo Jet 66: Aufbau, Funktionsweise und Energieumwandlungsprozesse einer Modellstrahlturbine, *www.frankturbine.de/doc/tj66.pdf*, 2002, accessed on 23 September 2005.

[3] Lake, J.P., King, P.I. and Rivir, R.B., Reduction of Separation Losses on a Turbine Blade with Low Reynolds Number, *AIAA Paper*, 1999-0242.

[4] Dorney, D.J., Lake, J.P., King, P.I. and Ashpis, D.E., Experimental and Numerical Investigation of Losses in Low-Pressure Turbine Blade Rows, *AIAA Paper*, 2000-0737.

[5] Lardeau, S., Leschziner, M.A. and Li, N., Modelling Bypass Transition with Low Reynolds Number Nonlinear Eddy Viscosity Closure, *Flow, Turbulence and Combustion*, Vol. 73, 2004, pp. 49-76.

[6] Suzen, Y.B. and Huang, P.G., Modeling of Flow Transition Using an Intermittency Transport Equation, *Journal of Fluids Engineering*, Vol. 122, 2000, pp.273-284.

[7] Menter, F.R., Langtry, R.B., Likki, S.R., Suzen, H.B. and Huang, P.G., A Correlation-Based Transition Model Using Local Variables. Part I - Model Formulation, *ASME Paper*, GT 2004-53452.

[8] Steelant, J. and Dick, E., Modelling of Bypass Transition with Conditioned Navier-Stokes Equations Coupled to an Intermittency Transport Equation, *International Journal for Numerical Methods in Fluids*, Vol. 23, 1996, pp. 193-220.

[9] Cho, J.R. and Chung, M.K., A k-ε-γ Equation Turbulence Model, *Journal of Fluid Mechanics*, Vol. 237, 1992, pp. 301-322.

[10] Wang, C. and Perot, B., Prediction of Turbulent Transition in Boundary Layers Using the Turbulent Potential Model, *Journal of Turbulence*, Vol. 3, No.1, 2002, pp. 1-15.

[11] Walters, D. K. and Leylek, J. H., A New Model for Boundary Layer Transition Using a Single-Point RANS Approach, *Journal of Turbomachinery*, Vol. 126, No.1, 2004, pp. 193-202.

[12] Walters, D.K. and Leylek, J.H., Simulation of Transitional Boundary-Layer Development on a Highly-Loaded Turbine Cascade with Advanced RANS Modeling, *ASME Paper*, GT 2003-38664.

[13] Walters, D. K. and Leylek, J. H., Computational Fluid Dynamics Study of Wake-Induced Transition on a Compressor-Like Flat Plate, *Journal of Turbomachinery*, Vol. 127, No.1, 2005, pp. 52-63.

[14] Holloway, D.S., Walters, D.K and Leylek, J.H., Prediction of Unsteady, Separated Boundary Layer over a Blunt Body for Laminar, Turbulent and Transitional Flow, *International Journal for Numerical Methods in Fluids*, Vol. 45, 2004, pp. 1291-1315.